Huygens Principle-based Microwave Brain Imaging through Finite Difference Time Domain

Moein Movafagh[1], Navid Ghavami[2,4], Gianluigi Tiberi[1,2,4], Sandra Dudley[1], Hideki Ochiai[3], Mohammad Ghavami[1]
[1]*School of Engineering, London South Bank University, London, UK*
[2]*UBT - Umbria Bioengineering Technologies, Perugia, Italy*
[3]*Department of Electrical and Computer Engineering, Yokohama National University, Japan*
[4] *UBT UK Division, W1B 3HH, London, UK*

***Abstract*—This paper investigates the application of Huygens principle (HP) in brain imaging. We employ simulation techniques, specifically the Finite Difference Time Domain (FDTD) method, in order to comprehensively evaluate the efficacy of this methodology in detecting strokes within the brain. The FDTD method is particularly noteworthy due to its straightforward implementation and high level of accuracy. Moreover, its compatibility with time domain analysis allows us to effectively incorporate time-varying sources. In order to demonstrate the effectiveness of HP procedure, we examine various scenarios in our simulations. The results provide compelling evidence of the considerable potential of HP imaging for the brain, highlighting its adaptability for a wide range of applications. These research findings yield valuable insights into the possibilities of using HP for brain imaging, laying the foundation for future advancements and innovation in the field of brain imaging for stroke detection.**

***Index Terms*—Huygens Principle, FDTD, Microwave Imaging**

I. Introduction

There is a significant amount of attention focused on the advancement of imaging techniques in the field of medicine. Recently, medical imaging technologies have the capability to generate clear and detailed tomographic reconstructions of living tissues through the utilization of various mediums. The most commonly employed methods include X-ray-based computed tomography (CT), and the RF technique of nuclear magnetic resonance imaging (MRI). However, each of these techniques possesses its own limitations. For instance, CT is highly proficient in capturing images of subjects with substantial contrast, but it entails a notable exposure to ionizing radiation, thereby restricting its usage [1]. Conversely, MRI has its own drawback in terms of scan duration, which can last up to 2 hours for a full-body scan. Throughout this time, patients are expected to maintain immobility within a relatively confined and claustrophobic setting.

Microwave imaging has garnered increasing interest in the past decades, particularly due to its potential for detecting brain strokes. This interest stems from the notable contrast in dielectric properties at microwave frequencies between various regions of the brain and areas affected by a stroke. Microwave technology offers several advantages, including the use of non-ionizing signals, cost-effectiveness, simplicity, and the ability to penetrate different mediums [2]. One of the key benefits of microwave imaging is its portability, allowing for the development of a portable detection system. This capability enables the initial diagnosis of critical and life-threatening conditions like strokes resulting from brain injuries, even while patients are being transported by ambulance to a hospital. This not only facilitates timely medical intervention but also saves crucial time in emergency situations [3].

Microwave imaging research can be broadly categorized into two main techniques: tomography and linear scattering methods. Tomographic image reconstruction involves solving a nonlinear inverse scattering problem to reconstruct an image of the dielectric properties [4]. This approach entails calculating both the radiating and non-radiating components of the induced currents, enabling efficient solutions for two-dimensional problems. In contrast, the linear scattering methods approach in microwave imaging focuses on a simpler computational problem by aiming to identify significant scatterers [5]. This technique avoids the complexities of tomography and instead concentrates on detecting important scatterers within the medium.

Among the linear scattering techniques, the Huygens principle (HP)-based technique stands out for its capability to detect inhomogeneities in dielectric materials in the frequency domain [6]. The utilization of HP in microwave imaging eliminates the necessity of solving complex inverse problems, thereby eliminating the need for matrix generation and inversion [7]. This approach offers simplicity and enables the assessment of distinguishability between various tissues or their differing conditions, ultimately resulting in the generation of contrast in the final image. Additionally, the use of Ultra Wide-band (UWB) technology allows for the comprehensive utilization of information in the frequency domain. By combining the information obtained from different frequencies, a coherent and consistent image can be constructed, harnessing the full potential of the frequency-based data. Notably, the HP technique requires a straightforward hardware setup, consisting of a single transmitting antenna and a single receiving antenna, coupled through a vector network analyzer. These antennas are rotated around the object of interest, collecting signals in a multi-bistatic manner.

Consequently, the methodology employed in this study enables the identification of significant scatterers within a given volume, along with their corresponding locations. The effectiveness of the technique has been validated through both analytical and numerical approaches, specifically on cylinders containing inclusions. The presented results showcase the efficacy of these methods in achieving accurate and reliable imaging outcomes. It is important to highlight that the numerical method utilizes the FDTD technique. The incorporation of FDTD allows for the consideration of various imaging scenarios, thereby enhancing the versatility and applicability of the methodology.

The structure of this paper is as follows. Section II provides an introduction to the HP-based procedure and discusses the fundamental principles of image formation using HP. In Section III, the simulation results obtained from both analytical and numerical methods are presented and analyzed. Finally, Section VI presents the concluding remarks of the paper, summarizing the key findings and contributions.

II. HUYGENS-PRINCIPLE-BASED PROCEDURE

A. Formulation

The concept described by Huygens' principle is as follows: "Each locus of a wave excites the local matter which reradiates secondary wavelets, and all wavelets superpose to a new, resulting wave (the envelope of those wavelets), and so on" [8]. In our study, we aim to apply this principle by using the known external field, E_{known}, as the locus of a wave. To effectively implement this strategy, we calculate the field inside a cylinder by superimposing the fields received by observation points (np).

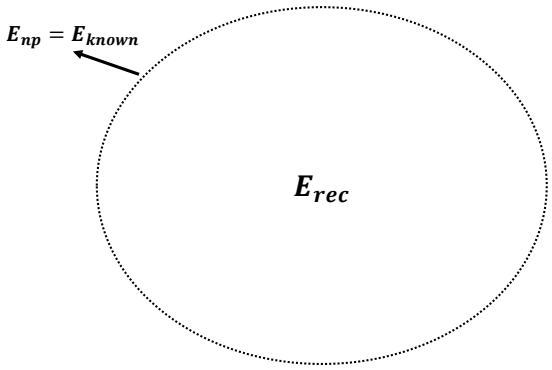

Fig. 1: HP Structure.

As can be seen in Fig. 1, let's assume that the field $E(\rho_{np})$ at the surface points $rx_{np} = \rho(a_0, \phi_{np}) = \rho_{np}$ is known. With the use of HP, it becomes straightforward to compute the electrical field within the phantom [7]:

$$E_{\text{rec}}(\rho, \phi; f) = \delta s \sum_{np=1}^{N_p} E(\rho_{np}) G(k_1 \left|\vec{\rho} - \vec{\rho_{np}}\right|) \qquad (1)$$

where δs is the spatial sampling:

$$\delta s = \frac{2\pi a_0}{N_p} \qquad (2)$$

and G is the Green function which is defined as:

$$G(k_1 \left|\vec{\rho} - \vec{\rho_{np}}\right|) = \frac{1}{4\pi \left|\vec{\rho} - \vec{\rho_{np}}\right|} e^{k_1 |\vec{\rho} - \vec{\rho_{np}}|} \qquad (3)$$

with k_1 representing the wavenumber for the media constructing the phantom.

B. HP-based Image Formation

In this study, we focus on a cylindrical object with radius a_0 that is located in free space and being illuminated by a transmitting line source tx_m operating at frequency f (Fig. 2). We make the assumption that the dielectric properties of the cylinder, including the dielectric constant ϵ_{r1} and conductivity σ_1, are already known. Furthermore, an inclusion with a higher dielectric constant than ϵ_{r1} is believed to be present within the cylinder. The objective of this research is to identify the inclusion's presence and location by only using the field measurements obtained outside of the cylinder.

Due to the mismatch between the dielectric properties of the inclusion and phantom, there is a significant alteration in the electrical field at the inclusion's boundary. As a result, utilizing the HP procedure to reconstruct the electrical field enables the identification and localization of the inclusion. Although this method is effective, it encounters several critical challenges that must be addressed. The electrical field amplitude of the background can often obscure the inclusion, rendering it undetectable. Hence, similar to other radar-based methods, various artifact removal techniques must be employed to eliminate the background and identify the inclusion.

One possible solution is to use multiple transmitters with different frequencies. Since the inclusion's location is fixed, we can create an image using different transmitters at various frequencies and then combine all of the images. This method takes advantage of the fact that the electrical field behaves similarly at the inclusion's boundaries for different frequencies and transmitters. However, the electrical field may behave differently in other parts of the phantom depending on the transmitter and frequency used. By combining the images, we can increase the detectability of the inclusion. Thus, the final image is obtained by the following equation:

$$E_{\text{rec}}^{\text{Final}}(\rho, \phi) = B \sum_{i=1}^{M} \sum_{j=1}^{F} \Delta f \left|E_{\text{rec}}(\rho, \phi; tx_i; f_j)\right|^2 \qquad (4)$$

where B and Δf represent the bandwidth and frequency sampling, respectively. M indicates the number of transmitters used, while F indicates the number of frequencies used for imaging.

In addition to the summation method mentioned earlier, there are other techniques available to improve the final image and remove the background effectively. Sohani et al. [9] introduced and investigated various methods for removing background, among which the local average subtraction (LAS)

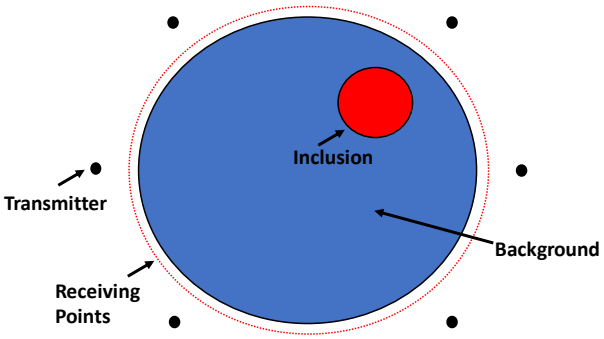

Fig. 2: Imaging Scenario structure.

artifact removal method [10] showed potential. LAS removes the background from final images by subtracting the received signal from the mean of all received signals.

$$E_{\text{recv}}^{\text{sub}}(\rho_{np}) = E_{\text{recv}}(\rho_{np}) - \text{avg}\{E_{\text{recv}}(\rho_{np}; tx_m)\} \quad (5)$$

As a result, the final image will be improved, and the inclusion can be easily detected and localized.

III. Simulation

In this section, we aim to evaluate the HP procedure using both analytical and numerical methods to generate an image of inclusion with arbitrary dielectric properties. To illustrate this, we examine a scenario involving a cylindrical phantom containing a material with a dielectric constant of $5\epsilon_0$. Inside the container, there is an inclusion with a dielectric constant of $50\epsilon_0$, as shown in Fig. 2. In this scenario, we employ six transmitters to facilitate the utilization of the artifact removal method, thereby enhancing the detection capability of the inclusion and enabling the generation of a high-quality image.

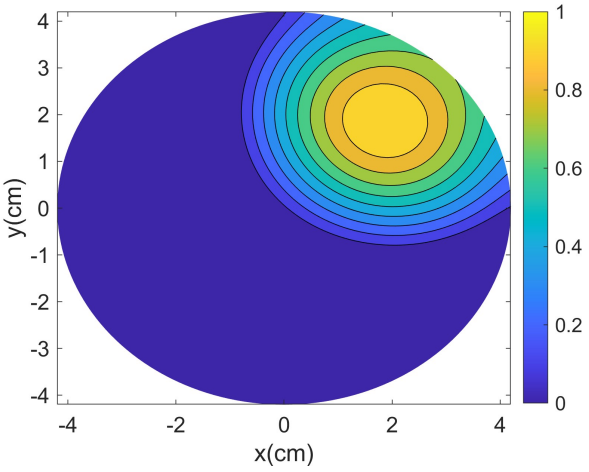

Fig. 3: The image of inclusion generated by using analytical method and HP technique.

In the analytical method, Maxwell's equations are solved in cylindrical form. By considering the boundary conditions between air, the phantom, and the inclusion, the coefficients of the solved equations are determined. This allows for the calculation of the electric field at the receiving points. By utilizing equations (1) and (4), the image of the inclusion can be generated successfully. The image depicted in Fig. 3 showcases the successful detection of the inclusion within the phantom using the HP approach through analytical simulation. This result demonstrates the capability of the HP method in accurately identifying the location of the inclusion inside the phantom, thereby validating its effectiveness in inclusion detection.

In the field of numerical analysis, several methods can be employed to simulate the electric field in a simulation environment. Notable examples include the Finite-Difference Time-Domain (FDTD) method [11], the Method of Moments (MoM) [12], and the Finite Element Method (FEM) [13]. In this study, we utilize the FDTD method to simulate the electric field within the phantom, enabling us to readily sample the electric fields surrounding the phantom. Therefore, we can conveniently employ the HP method to generate images and detect any inclusions present. Fig. 4 depicts a phantom that emulates the predefined phantom used in the analytic method (see Fig. 2). The dielectric properties of each region in the simulation environment are indicated by the corresponding colors. Fig. 5 shows the resulting image obtained through the utilization of the FDTD simulation and the HP method.

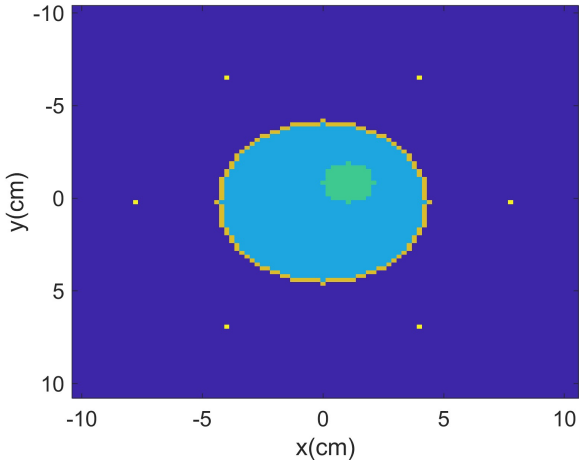

Fig. 4: The model phantom and inclusion used in numerical method.

Fig. 2 presents a simple model without any complex background elements. It serves as the basis for evaluating the effectiveness of HP. However, the primary objective of this study is to assess HP within more realistic scenarios. Thanks to FDTD technique, we can implement complex structures such as the brain and breast. To achieve this, an MRI image of a brain obtained from MRI simulator [14] is imported into the MATLAB environment and the dielectric properties of various sections of the brain are assigned based on the colors depicted in the model, as shown in Fig. 6.

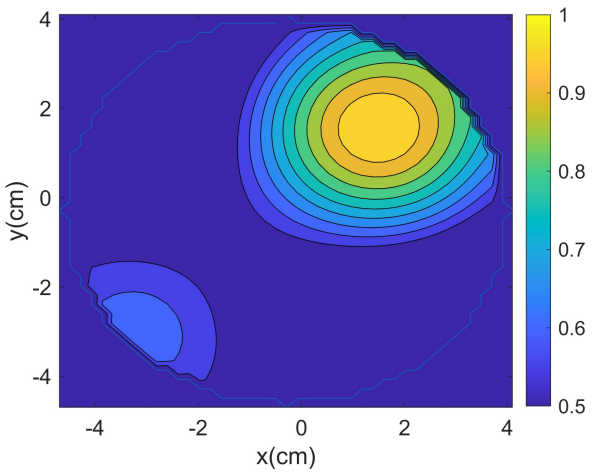

Fig. 5: The image of inclusion generated using the numerical method and HP technique.

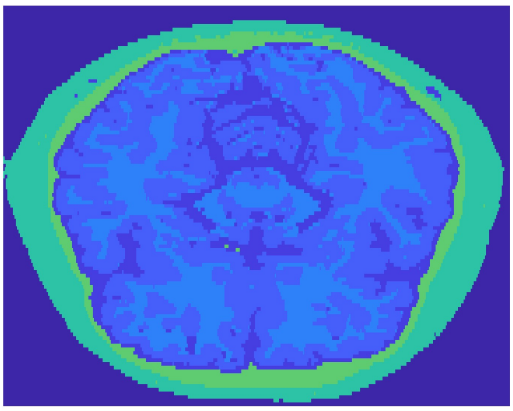

Fig. 6: the MRI image of brain imported into MATLAB environment.

To evaluate the effectiveness of the HP method in detecting a stroke within the brain, we introduce a setup and establish a configuration with transmitters and receiving points, adhering to the principles of HP (as illustrated in Fig. 7(a,c)). The dielectric properties of the brain are determined based on the information provided in Table I and the operation frequency of simulation is 650 MHz. Fig. 7(b,d) display images of two strokes with different locations, which are detectable within the brain. As evident from Fig. 7(a,c), the representation shows a perfect resemblance to an actual brain and exhibits greater complexity compared to the earlier depiction (Fig. 2). However, it is important to note that our simulation assumes both the air surrounding the brain and the brain tissue itself to be lossless, a simplification that does not reflect the real-world scenario.

	Skull	Avg	White matter	Grey matter	CSF	Stroke
ϵ_r	12.36	45.38	38.58	52.28	68.44	80

TABLE I: dielectric properties of brain layers assigned according to the color of each part.

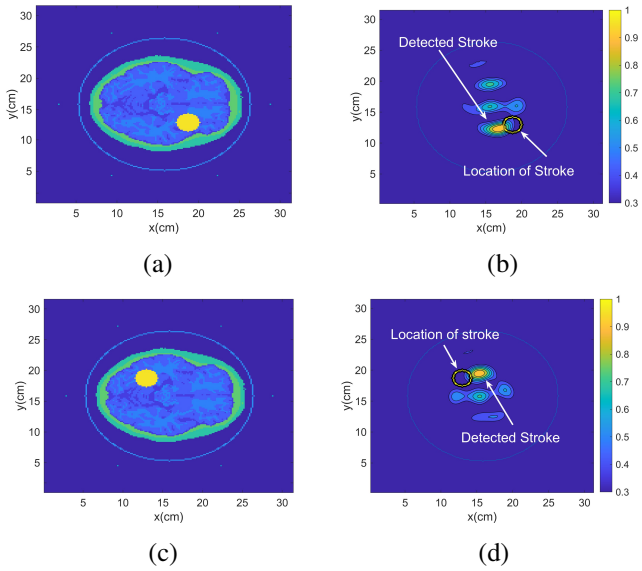

Fig. 7: (a),(c): The measurement setup used in MATLAB environment, (b),(d): The image created by using HP technique.

IV. Conclusions

This study aimed to explore the potential of using the HP technique for the detection of hemorrhagic stroke within the brain. To achieve this, we employed a series of steps within the MATLAB environment. Firstly, we imported an MRI scan of the brain and utilized the FDTD simulation method to accurately simulate the electrical field surrounding the brain. This simulation allowed us to leverage the HP technique effectively.

In our endeavor to achieve a realistic brain configuration, it is important to acknowledge that the air surrounding the brain and the brain itself as being lossless may not entirely mimic real-world conditions. Nevertheless, it represents an initial and positive stride towards attaining improved results applicable to real-world situations and actual brains.

The results obtained from the simulations demonstrate the HP technique's proficiency in detecting stroke, even within a more realistic brain structure.

V. Acknowledgment

This project has received funding from the European Union's Horizon 2020 research and innovation programme under the Marie Sklodowska-Curie grant agreement No. 872752. This project has also received funding from the European Union's Horizon 2020 research and innovation programme under grant agreement No. 101017098.

REFERENCES

[1] A. C. Kak and M. Slaney, *Principles of computerized tomographic imaging*. SIAM, 2001.

[2] E. M. Staderini, "Uwb radars in medicine," *IEEE aerospace and electronic systems magazine*, vol. 17, no. 1, pp. 13–18, 2002.

[3] D. Ireland and M. Bialkowski, "Microwave head imaging for stroke detection," *Progress In Electromagnetics Research M*, vol. 21, pp. 163–175, 2011.

[4] K. D. Paulsen and P. M. Meaney, "Nonactive antenna compensation for fixed-array microwave imaging. i. model development," *IEEE Transactions on Medical Imaging*, vol. 18, no. 6, pp. 496–507, 1999.

[5] B. Sohani, B. Khalesi, N. Ghavami, M. Ghavami, S. Dudley, A. Rahmani, and G. Tiberi, "Detection of haemorrhagic stroke in simulation and realistic 3-d human head phantom using microwave imaging," *Biomedical Signal Processing and Control*, vol. 61, p. 102001, 2020.

[6] B. Sohani, G. Tiberi, N. Ghavami, M. Ghavami, S. Dudley, and A. Rahmani, "Microwave imaging for stroke detection: Validation on head-mimicking phantom," in *2019 PhotonIcs & Electromagnetics Research Symposium-Spring (PIERS-Spring)*. IEEE, 2019, pp. 940–948.

[7] N. Ghavami, G. Tiberi, D. J. Edwards, and A. Monorchio, "Uwb microwave imaging of objects with canonical shape," *IEEE Transactions on Antennas and Propagation*, vol. 60, no. 1, pp. 231–239, 2011.

[8] P. Enders, "Huygens' principle as universal model of propagation," *Latin-American Journal of Physics Education*, vol. 3, no. 1, p. 4, 2009.

[9] B. Sohani, J. Puttock, B. Khalesi, N. Ghavami, M. Ghavami, S. Dudley, and G. Tiberi, "Developing artefact removal algorithms to process data from a microwave imaging device for haemorrhagic stroke detection," *Sensors*, vol. 20, no. 19, p. 5545, 2020.

[10] M. A. Elahi, M. Glavin, E. Jones, and M. O'Halloran, "Artifact removal algorithms for microwave imaging of the breast," *Progress In Electromagnetics Research*, vol. 141, pp. 185–200, 2013.

[11] E. Atef and V. Demir, "The finite difference time domain method for electromagnetics: With matlab simulations," 2009.

[12] M. M. Ney, "Method of moments as applied to electromagnetic problems," *IEEE transactions on microwave theory and techniques*, vol. 33, no. 10, pp. 972–980, 1985.

[13] J.-M. Jin, *The finite element method in electromagnetics*. John Wiley & Sons, 2015.

[14] "Brainweb - a web-based simulation brain database," https://brainweb.bic.mni.mcgill.ca/brainweb/.